BIOCHEMISTRY
including biophysical chemistry & molecular biology

Article

Action and Timing of BacC and BacD in the Late Stages of Biosynthesis of the Dipeptide Antibiotic Bacilysin

Jared B. Parker, and Christopher T. Walsh

Biochemistry, **Just Accepted Manuscript** • DOI: 10.1021/bi3016229 • Publication Date (Web): 14 Jan 2013

Action and Timing of BacC and BacD in the Late Stages of Biosynthesis of the Dipeptide Antibiotic Bacilysin

Jared B. Parker and Christopher T. Walsh*

Department of Biological Chemistry and Molecular Pharmacology

Harvard Medical School, 240 Longwood Ave, Boston, MA 02115

† This work was supported in part by National Institutes of Health Grant GM20011 (C.T.W.).

* To whom correspondence should be addressed: Email: Christopher_Walsh@hms.harvard.edu; Phone: 617.432.1715; Fax: 617.432.0483.

[1]Abbreviations: H_2HPP, dihydro-4-hydroxyphenylpyruvate; H_4HPP, tetrahydro-4-hydroxyphenylpyruvate; H_4Tyr, tetrahydrotyrosine; HPP, 4-hydroxyphenylpyruvate; LC/MS, liquid chromatography/mass spectrometry; NMR, nuclear magnetic resonance; gCOSY, gradient homonuclear correlation spectroscopy; gHSQC, gradient heteronuclear single-quantum coherence; gHMBC, gradient heteronuclear multiple bond coherence; HPLC, high-performance liquid chromatography; D_2O, deuterium oxide; *B. subtilis*, *Bacillus subtilis*; L-Ala, L-alanine; ATP, adenosine triphosphate; cPCR, colony-polymerase chain reaction; gDNA, genomic DNA; LB, Luria Broth; LC/MS, liquid-chromatography/mass spectrometry; PA media, Perry-Abraham media.

ABSTRACT

Biosynthesis of the dipeptide antibiotic bacilysin, encoded by the seven *B. subtilis* genes *bacA-G*, involves diversion of flux from prephenate to the noncognate amino acid anticapsin. The anticapsin warhead is then ligated to the *C*-terminus of L-alanine to produce mature bacilysin. We have previously noted the formation of two diastereomers of tetrahydrotyrosine (4*S*- and 4*R*-H_4Tyr) by tandem action of the four purified enzymes BacABGF. BacC (oxidase) and BacD (ligase) have been hypothesized to be remaining late stage enzymes in bacilysin biosynthesis. Using a combination of BacCD *in vitro* studies, *B. subtilis* deletion mutants, and isotopic feeding studies, we were able to determine that the H_4Tyr diastereomers are actually shunt products that are not on-pathway to bacilysin biosynthesis. Dihydroanticapsin and dihydrobacilysin accumulate in extracts of a Δ*bacC* strain and are processed to anticapsin and then bacilysin on addition of BacC and BacD, respectively. These results suggest the epoxide group in bacilysin is installed in an earlier step of bacilysin biosynthesis, while BacC oxidation of the C_7-hydroxyl followed by BacD ligation of anticapsin to L-Ala are the penultimate and ultimate steps of bacilysin biosynthesis.

INTRODUCTION

Bacilysin, the dipeptide of L-Ala ligated to the *N*-terminus of anticapsin (epoxycyclohexanonyl-Ala) (Figure 1A), is a Trojan Horse antibiotic excreted by some *Bacillus* species. [1, 2] Once bacilysin is transported into a neighboring cell, anticapsin can be freed by peptidase action. Free anticapsin inside a susceptible bacterial or fungal cell is a time-dependent, irreversible inactivator of the glutaminase domain of glucosamine synthetase [3, 4] (Figure S1). The blockade of GlcNAc formation leads to interdiction of cell wall biosynthesis and subsequent cell demise.

The seven-gene region *bacA-G* in producing *Bacillus* strains has been identified by genetic studies [1, 5] as the biosynthetic gene cluster responsible for bacilysin production (Figure 1, inset). In biochemical studies, we have previously established that BacABGF are four enzymes that act in tandem to divert some of the flux of prephenate away from production of L-Phe and L-Tyr into a four-step pathway leading to both 2*S*, 4*S*, 7*R*- and 2*S*, 4*R*, 7*R*-tetrahydrotyrosine (H_4Tyr) diastereomers [6-9] (Figure 1B). BacE is a proposed dipeptide permease involved in host resistance by pumping bacilysin from the intracellular to the extracellular environment [1]. In this work we evaluate the remaining two proteins BacC and BacD for their roles in the late stages of the bacilysin assembly pathway.

Bioinformatic analysis predicts BacC should be in the NAD^+-dependent oxidoreductase family, as is BacG. We have recently shown that BacG acts to reduce the 3*E*- and 3*Z*-*ex*-dihydrohydroxyphenylpyruvate (H_2HPP) geometric isomers to

the 2*S*, 4*R*, 7*R*- and 2*S*, 4*S*, 7*R*-diastereomers of H_4HPP, respectively, via conjugate hydride addition [8] (Figures S2A and S2B). Another obvious redox step in the formation of anticapsin is oxidation of the C_7-hydroxyl group found in prephenate to the ketone moiety found in anticapsin. We show here that purified BacC with NAD^+ cofactor will dehydrogenate the hydroxyl group in the 4*S*- but not the 4*R*-H_4Tyr diastereomer, consistent with the known 4*S* stereochemistry in anticapsin. Addition of purified BacD (promiscuous dipeptide ligase) [10, 11], ATP, and L-Ala to such BacC incubations yields a L-Ala-L-4*S*-cyclohexenonyl-Ala dipeptide.

To shed light on the timing of epoxidation at the C_5-C_6 double bond vs. oxidation of the C_7 hydroxyl to ketone vs. dipeptide ligation, we have undertaken two approaches. One was construction of a Δ*bacC B. subtilis* strain to characterize accumulating intermediates. The second approach involved feeding *B. subtilis* with isotopically labeled versions of 4*S*- and 4*R*-H_4Tyr along with isotopically labeled earlier pathway intermediates, 3*Z*- and 3*E*-*ex*-H_2HPP. Of these four compounds, only feeding with 3*E*-*ex*-H_2HPP yields isotopically labeled bacilysin/anticapsin, suggesting both the H_4Tyr diastereomers and 3*Z*-H_2HPP may be *in vitro* shunt products in the absence of the (still unidentified) expoxidase. Additionally, we conclude that C_5-C_6 double-bond epoxidation occurs before C_7 hydroxyl oxidation to the ketone, which is immediately followed by dipeptide ligation to form mature bacilysin.

MATERIALS AND METHODS

Materials and Instrumentation. Prephenic acid barium salt, β-nicotinamide adenine dinucleotide hydrate (NAD^+), β-nicotinamide adenine dinucleotide reduced disodium salt hydrate (NADH), L-phenylalanine, L-alanine, adenosine 5′-triphosphate disodium salt, and Dowex resin were purchased from Sigma-Aldrich. Deuterium oxide (99.9%) (D_2O) and 3-[^{13}C]-L-alanine (99%) was purchased from Cambridge Isotope Laboratories. DNA oligonucleotide primers were obtained without purification from Integrated DNA Technologies. Restriction endonucleases and T4 DNA ligase were obtained from New England BioLabs. *Bacillus subtilis* sp. 168 genomic DNA and *B. subtilis* sp. PY79 cells were obtained from ATCC. ^{1}H one-dimensional and two-dimensional NMR spectra were recorded at 25 °C on a Varian VNMRS 600 MHz spectrometer equipped with a triple-resonance probe. ^{13}C one-dimensional NMR spectra were recorded on a Varian MR 400 MHz spectrometer (100.497 MHz for ^{13}C) equipped with a ONE NMR probe. NMR data were processed with ACD/Laboratories software. High-resolution LC/MS data were collected on an Agilent Technologies 6520 Accurate-Mass Q-TOF LC/MS system and analyzed (including integration) using the accompanying Mass Hunter Qualitative Analysis software. HPLC was performed on a Beckman Coulter System Gold instrument. UV-vis measurements were collected using a Cary 50 BIO UV-vis spectrophotometer and analyzed using the accompanying software. DNA sequencing was performed by Genewiz. Purification of plasmid DNA and PCR amplified dsDNA was performed using kits from Qiagen.

Cloning, Expression, and Purification of the Enzymes BacABCDFG. The cloning of plasmids for production of BacABGF has been previously described [7, 8]. The gene for BacC (*ywfD*) was amplified from *B. subtilis* sp. 168 genomic DNA via PCR using primers encoded with *BamHI* and *XhoI* restriction sites (5′-AATCCGGATCCATGATCATGAACCTCACC-3′ and 5′-AATTCTCGAGCTATTGTGCGGTGTATCCTCC-3′, respectively). The gene for BacD (*ywfE*) was amplified from *B. subtilis* sp. 168 genomic DNA via PCR using primers encoded with *NdeI* and *XhoI* restriction sites (5′-CGGCAGCCATATGGAGAGAAAAACAGTATTGGTCA-3′ and 5′-GGTGCTCGAGTCATACTGGCAGCACATACTTTGCC-3′, respectively). Each amplified gene was ligated into vector pET-28a (Novagen) such that the target protein would be expressed as an *N*-terminally tagged His_6-fusion. The ligated plasmid was transformed into chemically competent TOP10 *E. coli* cells (Invitrogen) and proper gene insertion was confirmed by DNA sequencing of the purified plasmid DNA. The sequence-confirmed plasmid was then transformed into chemically competent BL21(DE3) *E. coli* cells for protein expression. Protein expression and purification of BacC and BacD was performed exactly as previously reported for BacA [7]. Protein purity of both BacC and BacD was judged to be > 95% from SDS-PAGE analysis on an Any *k*D TGX gel (BioRad) with visualization by coomassie blue staining (Figure S3). The concentration of each protein was determined by UV-vis absorbance using the following extinction coefficients (ε_{280nm}) calculated from the protein primary sequence using the ExPASy Bioinformatics Research Portal: 18 450 M^{-1} cm^{-1} for BacC and 40 340 M^{-1} cm^{-1} for BacD. Extinction coefficients for BacABGF have been

previously reported [7, 8]. Protein stocks were flash frozen in liquid N_2 and stored at -80 °C until use.

Construction of Δ*bacB* and Δ*bacC B. subtilis* PY79 genomic deletion mutants. Markerless Δ*bacB* and Δ*bacC* deletions were made in the *B. subtilis* PY79 genome with use of the pMiniMAD plasmid [12] (Figure S4). Plasmid pMiniMAD-Δ*bacB* was constructed by PCR amplifying the 800 bp genomic regions upstream and downstream of the *bacB* gene from *B. subtilis* 168 gDNA using the primers SAM-1 with SAM-2 and SAM-3 with SAM-4, respectively (Table S1) [13]. The two PCR amplified dsDNA fragments were gel purified and ligated into the pMiniMAD plasmid cleaved with *BamHI* (3-piece ligation) using the one-step isothermal DNA assembly method of Gibson and coworkers [14]. The isothermal assembly mastermix used to accomplish the ligation was made in-house according to the published recipe [14]. Plasmid pMiniMAD-Δ*bacC* was constructed by PCR amplifying the 500 bp genomic regions upstream and downstream of the *bacC* gene from *B. subtilis* 168 gDNA using the primers JBP-1 with JBP-2 and JBP-3 with JBP-4, respectively (Table S1). The remainder of the pMiniMAD-Δ*bacC* construction was identical to the pMiniMAD-Δ*bacB* assembly described above. The ligated plasmids were transformed into *E. coli* TOP10 chemically competent cells (Invitrogen), positive transformants selected on LB-agar containing 50 μg/mL ampicillin, and plasmid DNA was purified. Sequencing of both DNA strands confirmed proper construction of the mature pMiniMAD plasmids. The sequence confirmed plasmids were individually transformed into chemically competent *recA*+ BL21(DE3) cells

(Invitrogen) and plasmid DNA purified from these cells was used for *B. subtilis* transformation.

Deletion of the target genes from the *B. subtilis* genome was accomplished by double-crossover homologous recombination, performed in two single-crossover steps (Figure S4). The pMiniMAD plasmid containing the appropriate deletion homology (either Δ*bacB* or Δ*bacC*) was transformed into *B. subtilis* PY79 cells (single-crossover integration step) using a one-step competence protocol provided by the Rudner lab at HMS. To transform, a freshly streaked colony of *B. subtilis* was inoculated into 1 mL of MC medium (100 mM potassium phosphate pH 7.0, 3 mM sodium citrate, 2% glucose, 22 mg/mL ferric ammonium citrate, 0.1% casein hydrolysate, 0.2% potassium glutamate, and 3 mM magnesium sulfate) and grown for 4 h at 37 °C in a roller drum traveling at 60 rpm. 2 μL of pMiniMAD plasmid (at various dilutions) were mixed with 200 μL of the 4 h culture and re-incubated in the roller drum for 2 h followed by plating on LB-agar + MLS and incubation at 37 °C for 20 h. Because pMiniMAD contains an erythromycin resistance cassette, positive transformants were identified by selecting for resistance to MLS antibiotic (1 μg/mL erythromycin and 25 μg/mL lincomycin). The second-crossover was accomplished by growing a single-crossover *B. subtilis* transformant in LB broth (containing no antibiotics) at 21 °C (pMiniMAD contains a temperature sensitive origin of replication) for 24 h, diluting the culture into fresh LB broth, and repeating the growth/dilution process twice more. Replication initiation stimulates homologous recombination and the integrated DNA has two regions of homology. Accordingly,

recombination between one of these two regions and the homologous chromosomal region will "loop-out" the plasmid in a manner that regenerates the wild-type gDNA configuration, while recombination of the other integrated homologous region with the corresponding chromosomal region will result in the second-crossover and give expulsion ("loop-out") of the pMiniMAD backbone and target gene, creating the desired deletion (Figure S4). Second-crossover ("loop out") candidate colonies (plated on LB-agar) could be initially identified by loss of resistance to MLS antibiotic. Antibiotic sensitive colonies were then screened by cPCR to confirm the deletion junctions.

Production and LC/MS analysis of bacilysin and associated intermediates from *B. subtilis* PY79 strains. For general bacilysin production, *B. subtilis* PY79 WT cells were grown in PA minimal media [15] . One liter of PA media in H_2O contained the following components: 1.1 g potassium phosphate monobasic; 0.55 g of magnesium sulfate heptahydrate; 0.55 g of potassium chloride; 4.4 g of L-glutamic acid monosodium salt monohydrate; 13.7 g sucrose; 0.1 g trisodium citrate dihydrate; 0.1 g iron(III) chloride hexahydrate; 1 mL of oligodynamic solution [16] ; pH to 7.0 using sodium hydroxide. The media was sterilized via filtration using a 0.22 μm PES membrane.

Small-scale bacilysin production for LC/MS analysis was accomplished by inoculating a 5 mL culture of PA media with a single colony of *B. subtilis* PY79 WT cells from a freshly streaked LB-agar plate. The culture was incubated at 30 °C in a roller drum traveling at 60 rpm for 48 h. The culture was then clarified via

centrifugation at 3000*g* for 15 minutes at 4 °C. The pellet was disposed and the bacilysin containing supernatant was kept for further processing by one of two ways as will be indicated in the figure legend of each reported experiment. Either the supernatant was diluted 2-fold with H_2O, frozen, and lyophilized to dryness; or the supernatant was subjected to a Dowex purification. For Dowex purification, the supernatant was first diluted 2-fold in ice-cold ethanol, centrifuged as described above, and the pellet discarded. The supernatant was gravity fed through a 2 x 1 cm Dowex 50WX8-200 hand-poured column equilibrated in 50/50 ethanol/H_2O. Unbound material was washed away with 5 mL of H_2O and bound compounds were eluted with 2 mL of 4% ammonium hydroxide (aqueous) into a vessel submerged in liquid N_2. The elution was immediately flash frozen and lyophilized to dryness. This small-scale growth/Dowex purification was also performed with *B. subtilis* PY79 Δ*bacB* and Δ*bacC* strains. Dowex purification of the Δ*bacC* culture yielded dihydrobacilysin and dihydroanticapsin products that had their epoxide hydrated. To avoid this fate the Δ*bacC* strain was re-grown and the supernatant was lyophilized without subjection to Dowex purification. Although this resulted in lower signal-to-noise ratio during LC/MS analysis (data not shown), the masses of dihydrobacilysin and dihydroanticapsin with the intact epoxide were obtained (Figure 2). All lyophilized samples were dissolved in ~ 1 mL of H_2O for loading onto the LC/MS.

LC/MS detection of bacilysin, anticapsin, dihydrobacilysin, and dihydroanticapsin was performed in positive detection mode with 0.1% formic acid spiked into Buffer A (H_2O) and Buffer B (acetonitrile). The mass spectrometer was

set to the following parameters: 2500 V capillary voltage; 350 °C drying gas at a flow-rate of 10 L/min; 30 psi nebulizer pressure; and 125 V fragmentor voltage. The LC was set to a flow-rate of 0.4 mL/min through a 50 x 2.1 mm 5 μ Hypercarb column. The sample loading volume was 3 μL and the compounds were eluted using the following LC program: 0% Buffer B for 1 min; 0 - 95% linear gradient of Buffer B over 10 min; 95 - 0% Buffer B linear gradient over 2 min, 0% Buffer B re-equilibration for 10 min before loading the next sample. Samples in which the mass signals saturated the detector were diluted in H_2O and re-run.

Production and purification of dihydroanticapsin hydrate for NMR analysis. To produce enough dihydroanticapsin to allow the collection of NMR spectra, a 500 mL culture of PA media (additionally buffered with 100 mM MOPS pH 6.8) was placed in a 2800 mL baffled flask and inoculated with a 5 mL starter culture grown in the same media. The starter culture had been inoculated with a freshly streaked colony of *B. subtilis* PY79 Δ*bacC* cells and grown for 16 h at 30 °C in a roller drum traveling at 60 rpm. After inoculation, the 500 mL culture was grown at 30 °C for 48 h with shaking at 200 rpm. The supernatant of the culture (containing dihydroanticapsin) was harvested via centrifugation at 3000*g* for 20 min at 4 °C. The pellet was discarded and the supernatant was diluted 2-fold with ice-cold ethanol. Nascent precipitate was removed by repeating the centrifugation described above and discarding the pellet.

The first step of purification consisted of loading the supernatant onto a 6 x 2.5 cm Dowex 50WX8-200 hand-poured column via gravity flow at room

temperature. The Dowex resin had been previously equilibrated in 50/50 ethanol/H_2O. Unbound material was washed away with 40 mL of H_2O. Bound compounds were eluted with 40 mL of 4% aqueous ammonium hydroxide into a vessel submerged in liquid N_2. After freezing, the elution was lyophilized to dryness.

For the next purification step, the lyophilized Dowex elution was dissolved in 3 mL of Buffer A (H_2O + 0.1% formic acid). 1 mL of this mixture was loaded onto a 100 x 21.2 mm Hypercarb 5 μ column equilibrated in Buffer A using a flow-rate of 4 mL/min (3 runs total). Bound components were eluted with a 0 - 95% linear gradient of Buffer B (acetonitrile + 0.1% formic acid) over 45 min. Fractions (4 mL) containing dihydroanticapsin hydrate were identified by LC/MS using the same method as described above for bacilysin analysis. Once identified, the fractions containing dihydroanticapsin hydrate were frozen and lyophilized to dryness.

The final purification step of dihydroanticapsin hydrate was identical to the purification described in the previous paragraph, except with Buffer A as 10 mM potassium phosphate pH 8 and Buffer B as neat acetonitrile. The fraction (3 mL) containing dihydroanticapsin hydrate was frozen, lyophilized to dryness, and dissolved in 300 μL of D_2O. The sample was placed in a 5 mm D_2O matched Shigemi tube and NMR spectral data (^1H, ^{13}C, ^1H-^{13}C HSQC, ^1H-^{13}C HMBC, ^1H-^1H COSY, ^1H-^1H NOESY) were collected at 25 °C. Water suppression was accomplished via pre-saturation and proton signals were referenced to the residual H_2O peak (4.79 ppm) [17]. Carbon peaks were referenced by spiking the NMR sample with 0.5 μL of acetonitrile and referencing to its methyl carbon signal (1.47 ppm) [17]. Pure

bacilysin was expressed and processed exactly as described for dihydroanticapsin except the initial supernatant was obtained from *B. subtilis* PY79 WT cells (Figure S15).

BacC and BacD reactions with 4*S*-and 4*R*-H_4Tyr. H_4Tyr diastereomer substrates were prepared in preparative amounts from potassium prephenate as previously described [8]. The concentrations of the substrates were determined from NMR proton spectra by referencing the integration of the C_7 proton signal of H_4Tyr to the proton signal of an internal standard of 1 mM sodium formate (Figure S5).

The ability of BacC to process 4*S*- and 4*R*-H_4Tyr was initially screened via a UV-vis assay monitoring the production of NADH at 340 nm. The reactions contained 4 mM NAD^+ and 2 mM H_4Tyr diastereomer in 50 mM potassium phosphate buffer pH 8.0. Each reaction was initiated via addition of 25 μM BacC, placed in a 1 cm quartz cuvette, and monitored for 30 seconds in the spectrophotometer at 20 °C.

The reactivity of BacC and BacD with the H_4Tyr diastereomers was further analyzed by LC/MS in negative detection mode using the same flow-rate, column, and LC method as the LC/MS analysis of bacilysin. However, in this experiment Buffer A and Buffer B contained 0.1% ammonium hydroxide instead of formic acid and the spectrometer parameters were set to the following: 3500 V capillary voltage; 300 °C drying gas at a flow-rate of 11 L/min; 30 psi nebulizer pressure; and 125 V fragmentor voltage. Reactions for this analysis contained 1 mM H_4Tyr, 3 mM L-Ala, 3 mM ATP, 3 mM NAD^+, and 5 mM $MgCl_2$ in 50 mM potassium phosphate

buffer pH 8.0. The reactions were initiated via the addition of 20 μM of BacC alone, BacD alone, or BacCD added simultaneously. After incubation at room temperature for 6 h, each 25 μL reaction was quenched by adding acetonitrile to 75% *v*/*v* and vortexing. H_2O was added to the quenched reactions to reduce the concentration of acetonitrile to 25% *v*/*v* to facilitate freezing. The reactions were frozen, lyophilized to dryness, re-dissolved in 120 μL of H_2O, centrifuged to pellet any insoluble material, and 3 μL of the supernatant was loaded onto the LC/MS for analysis.

Preparative scale reactions of BacD and BacCD were run with 4*S*-H_4Tyr to obtain product dipeptides for NMR analysis. The BacD reaction contained 6 mM 4*S*-H_4Tyr, 15 mM ATP, 15 mM L-Ala, 20 mM $MgCl_2$, 1 mM DTT, and 20 μM BacD in 500 μL of potassium phosphate buffer pH 8.0. The BacCD reaction was identical to the BacD reaction except with the addition of 15 mM NAD^+, 30 μM BacC, and the concentration of BacD was decreased to 10 μM. Both reactions were incubated at room temperature for 12 h before being quenched via addition of acetonitrile to 30% *v*/*v*, frozen in liquid N_2, and lyophilized to dryness. The dried reactions were re-dissolved in 1 mL of Buffer A for purification (10 mM potassium phosphate buffer pH 8). The reaction mixtures were centrifuged to pellet insoluble material and the supernatants were loaded (individually) onto a 100 x 10 mm 5μ Hypercarb column equilibrated in Buffer A at a flow-rate of 1.5 mL/min. Bound compounds were eluted with a linear gradient of acetonitrile (no additives) and fractions were analyzed for the appropriate product via LC/MS in negative detection mode as described above for the analysis of the small-scale BacCD reactions. 3 mL of

fractions containing the desired compounds were frozen, lyophilized to dryness, and dissolved separately in 300 μL of D_2O. The dissolved compounds were analyzed by NMR spectroscopy as described above for dihydroanticapsin hydrate.

BacC and BacD reactions with *B. subtilis* PY79 Δ*bacC* lyophilized extracts. The Δ*bacC* extract used as substrate was identical to that described above (without Dowex processing) that contained masses of dihydrobacilysin and dihydroanticapsin with the intact epoxide (Figure 2). Each 50 μL reaction contained 33 μL of Δ*bacC* extract spiked with 2 mM NAD^+, 2 mM L-Ala, 2 mM ATP, and 50 mM potassium phosphate pH 8.0. The reactions were initiated with 20 μM of BacC, BacD, or BacCD simultaneously. The reactions were incubated, quenched, and prepared for LC/MS analysis exactly as described above for the BacCD reactions with H_4Tyr. However, the actual LC/MS analysis was identical to the positive detection mode method used to analyze the original Δ*bacC* extract (described above).

Feeding studies with isotopically labeled [^{13}C]-H_4Tyr and [^{2}H]-*ex*-H_2HPP diastereomers. Purified 4*R*- and 4*S*-[^{13}C]-H_4Tyr diastereomers were prepared from 3, 5, 5'-[^{13}C]-prephenate (non-uniformly labeled) as previously described for the generation of unlabeled H_4Tyr diastereomers. The 3, 5, 5'-[^{13}C]-prephenate was enzymatically prepared from 2, 6, 9-[^{13}C]-chorismate as previously described [7]. The concentration of both [^{13}C]-H_4Tyr diastereomers was determined by NMR spectroscopy by referencing to an internal standard of sodium formate as described above for unlabeled H_4Tyr. The extents of [^{13}C]-labeling of the H_4Tyr diastereomers

were determined by LC/MS using the negative detection mode method described above (Figure S6).

Purified 3*E*- and 3*Z*-[^{2}H]-*ex*-H_2HPP diastereomers were prepared from reactions of prephenate in 95% D_2O with either BacAB or AerDE, respectively, as previously described [8]. The concentration of each diastereomer was determined via UV-vis spectroscopy using previously reported extinction coefficients [8]. The extents of [^{2}H]-labeling of the *ex*-H_2HPP diastereomers were determined by LC/MS using the negative detection mode method described above (Figure S6).

4*R*- and 4*S*-[^{13}C]-H_4Tyr diastereomers were added (separately) to 5 mL cultures of PA media (additionally buffered with 100 mM MOPS pH 6.8) at a final concentration of 1 mM. The cultures were inoculated with a freshly streaked colony of *B. subtilis* PY79 WT and Δ*bacB* cells (separately) and incubated at 30 °C for 48 h in a roller drum traveling at 60 rpm. The culture was clarified via centrifugation (as described above) and the supernatant was diluted 2-fold into H_2O before being froze and lyophilized to dryness. The dried supernatant was resuspended in 1 mL of H_2O and analyzed via LC/MS using the positive detection mode method described above. To ensure that *B. subtilis* could take up labeled amino acids under our experimental conditions, this feeding experiment was repeated with *B. subtilis* PY79 WT cells being fed with 3-[^{13}C]-L-alanine (99% labeling uniformity) instead of [^{13}C]-H_4Tyr. Because L-Ala can be transaminated *in vivo* to yield pyruvate, we saw multiple ^{13}C labels incorporated into bacilysin indicating L-Ala was accepted into *B. subtilis* cells (Figure S7).

3*E*- and 3*Z*-[^{2}H]-*ex*-H_2HPP diastereomers were added (separately) to 5 mL cultures of PA media at a final concentration of 1 mM. (MOPS was not added to this media as we found the high concentration of MOPS present in the [^{13}C]-H_4Tyr feedings to saturate the detector.) The cultures were inoculated with a freshly streaked colony of *B. subtilis* PY79 WT, Δ*bacB,* and Δ*bacC* cells (separately). The cultures were grown at 37 °C for 24 h in a roller drum traveling at 60 rpm. The cultures were then clarified, the supernatant processed using Dowex 50WX8-200 resin, and LC/MS analyzed in positive detection mode exactly as described above for the analysis of bacilysin from small-scale *B. subtilis* PY79 cultures.

Because previous data had shown that the deuteriums in the [^{2}H]-*ex*-H_2HPP diastereomers can exchange with protons in H_2O upon BacB action [7, 8], the temperature of the incubations in the above paragraph was increased relative to that in the H_4Tyr feeding incubations (described above) so that a shorter incubation time could be employed to limit "washing out" of the deuterium signal. To ensure that the new incubation conditions would provide the same qualitative result, albeit cleaner, as the conditions used for the [^{13}C]-H_4Tyr feedings, 3*E*-[^{2}H]-*ex*-H_2HPP (1 mM) was fed to a 5 mL *B. subtilis* PY79 WT culture and incubated/processed exactly as for the [^{13}C]-H_4Tyr feedings (Figure S8).

RESULTS AND DISCUSSION

Evidence for 5,6-epoxy-7-hydroxycyclohexyl-Ala (dihydroanticapsin) in *B. subtilis* Δ*bacC* extracts. In parallel with *in vitro* studies on purified BacC described in a subsequent section, we undertook construction of a clean Δ*bacC*

deletion mutant of the bacilysin-producing *B. subtilis* PY79 strain to evaluate accumulating intermediates. The Δ*bacC* deletion mutant was constructed by double-crossover homologous recombination using the pMiniMAD plasmid [12]. To obtain the deletion, two regions of homology were cloned into pMiniMAD: 1) the 500 bp sequence immediately upstream of *bacC* joined directly to 2) the 500 bp sequence located immediately downstream of *bacC*. However, because the stop codon of *bacB* (TGA) overlaps the start codon of *bacC* (ATG), the stop codon of *bacB* was mutated from TGA to TAA so the start codon of *bacC* (now ATA) would be disrupted to eliminate nonsense transcripts. These two regions of homology were ligated together and into the pMiniMAD plasmid using the method of Gibson et al. [14] such that cloning scars were not introduced. The plasmid was then transformed into *B. subtilis* PY79 and positive transformants were identified via the erythromycin resistance cassette present in the pMiniMAD backbone (this integration event is single-recombination: integration of the entire plasmid into the chromosome (Figure S4)). Individual colonies were inoculated in LB liquid cultures without antibiotic and incubated in attempt to accomplish the second-recombination. The second-recombination removes the plasmid backbone, resistance cassette, and gene of interest from the chromosome. After several rounds of dilution and re-growth, culture was plated on LB agar without antibiotics. Colonies that successfully completed the second-recombination were initially identified via replica plating on LB-agar containing erythromycin, and then confirmed by colony-PCR followed by sequencing of the colony-PCR dsDNA product.

B. subtilis PY79 Δ*bacC* cells (and WT cells as control) were grown in minimal media and the cell mass and spent media (5 mL) were separated by centrifugation. The cell mass was discarded while the supernatant was frozen and lyophilized. The lyophilized media extract was then examined for anticapsin, bacilysin, and any dihydro-intermediates that might accumulate from loss of the predicted C_7-hydroxyl oxidase activity of BacC (Figure 2A). High-resolution LC/MS analyses (Figures 2B and 2C) showed the WT extract contained a significant amount of bacilysin (calc. mass: 271.1288; observed: 271.1296) and a minor amount of anticapsin (calc. mass: 200.0917; observed: 200.0921), but the Δ*bacC* extract did not possess detectable amounts of either. However, the Δ*bacC* extract did contain accumulated amounts of masses corresponding to dihydroanticapsin (calc. mass: 202.1074, observed: 202.1072) and dihydrobacilysin (calc. mass: 273.1445; observed: 273.1446), which contain the intact epoxide but possess a C_7-hydroxyl moiety in place of the C_7-ketone found in mature anticapsin and bacilysin (Figure 2A). This finding is consistent with BacC assignment as the dehydrogenase used to oxidize the C_7-hydroxyl, and strongly suggests that BacC oxidation occurs sometime after the epoxidation of the cyclohexenol double-bond.

To support the existence of the dihydroanticapsin/dihydrobacilysin intermediates suggested above by the LC/MS data, a fermentation of the Δ*bacC* deletion strain was scaled up in an effort to obtain sufficient materials for NMR characterization. 500 mL of *B. subtilis* Δ*bacC* culture was harvested and after discarding the cell mass, the spent media was subjected to an initial purification on a

hand-poured Dowex 50WX8-200 cation-exchange column. Bound compounds were eluted with a 4% solution of aqueous ammonium hydroxide and then subjected to further purification on a preparative Hypercarb HPLC column. Even though dihydrobacilysin was already an initial minor component compared to dihydroanticapsin (Figure 2B), after the acidic purification on the Dowex and Hypercarb resins essentially all of the dihydrobacilysin dipeptide was hydrolyzed to the amino acid (data not shown). Additionally, the epoxide of dihydroanticapsin became irreversibly hydrated to 5, 6, 7-trihydroxycyclohexyl-Ala that we termed dihydroanticapsin hydrate (calc. mass: 220.1179; observed: 220.1183) (Figure 3, Table S2). As shown in Figure 3, the structure of dihydroanticapsin hydrate was definitively determined by ^{1}H-NMR spectroscopy, fully consistent with the LC/MS data for the Δ*bacC* culture extracts presented above. Only a trace amount of this trihydroxy intermediate is detectable in the *B. subtilis* WT strain with the functional *bacC* gene (when processed with Dowex) (Figure S9A). Although a ^{1}H – ^{1}H NOESY spectrum was collected in attempt to determine the stereochemistry of the three hydroxyl groups present in dihydroanticapsin hydrate, spectral overlap between H_5, H_6, H_7 and H_{3b}, H_4 made this task impossible (Figure 3).

Purified BacC oxidizes 2*S*, 4*S*, 7*R*- but not 2*S*, 4*R*, 7*R*-H$_4$Tyr. Overproduction of *B. subtilis* BacC with an *N*-terminal His$_6$-tag was carried out in *E. coli* BL21 (DE3) cells, yielding 16 mg of purified, soluble BacC protein per liter of culture (Figure S3). Incubations of BacC and NAD$^+$ cofactor with the purified hydrate of dihydroanticapsin yielded unaltered substrate. Although we were not able to purify the presumed *in vivo* BacC substrate (dihydroanticapsin), due to

reactivity of the epoxide, we did possess mg quantities of 2*S*, 4*S*, 7*R*- and 2*S*, 4*R*, 7*R*-H_4Tyr diastereomers, remaining from our previous study [8], to test as potential surrogate substrates. (For simplicity, 2*S*, 4*S*, 7*R*-H_4Tyr will be abbreviated as 4*S*-H_4Tyr and 2*S*, 4*R*, 7*R*-H_4Tyr will be abbreviated as 4*R*-H_4Tyr for the remainder of this manuscript.) When 2 mM of these two substrates were individually exposed to 25 μM of purified BacC and 4 mM NAD^+ cofactor, the incubation of the 4*S*-H_4Tyr diastereomer showed 100-fold higher velocity than the incubation with the 4*R*-H_4Tyr diastereomer, as noted by the increase in light absorption at 340 nm (Figure 4A). (It is possible that the detected velocity of the 4*R*-H_4Tyr incubation is actually due to 4*S*-H_4Tyr contamination from how the H_4Tyr diastereomers are prepared [8].) Additionally, LC/MS analysis (positive detection mode) of the 4*S*-H_4Tyr reaction showed the appearance of a new mass corresponding to H_4Tyr with an oxidized C_7 hydroxyl, cyclohexenonyl-Ala (calc. mass: 184.0968; observed 184.0969) (Figure S10B). LC/MS analysis of the 4*R*-H_4Tyr reaction showed no detectable amount of new product (Figure S10A)

Given that anticapsin has 4*S* stereochemistry, it was gratifying to observe that BacC oxidized the 4*S*-H_4Tyr diastereomer but possessed negligible activity with the 4*R*-H_4Tyr diastereomer (Figure 4A). We anticipated the product enone might be susceptible to both intermolecular addition of exogenous nucleophiles as well as intramolecular capture by its own amino group [18]. Indeed, prolonged incubations of BacC with 4*S*-H_4Tyr to obtain NMR quantities of the BacC product yielded multiple product peaks as observed by LC/MS (as also seen in Figure S10B). The identity of those metabolites is the subject of a further study that will be reported

separately and relates to the formation of the bicyclic 2-carboxy-6-hydroxyoctahydroindole scaffold found in cyanobacterial aeruginosin peptide toxins [19, 20] . As detailed below, we turned to a coupled assay with purified BacD ligase enzyme to generate a stable dipeptide product to enable further characterization.

Action of BacD as an L-Ala-L-amino acid dipeptide ligase. Bioinformatics predicts that BacD is in the ADP-forming dipeptide ligase superfamily. In support of this prediction, workers have reported initial kinetic studies of BacD as an L-Ala-L-X promiscuous dipeptide ligase with potential practical utility [10, 11] . They had not, however, probed specificity for the possible *in vivo* substrates of BacD (i.e. X= anticapsin, H_4Tyr, its C_7-oxidation product cyclohexenonyl-Ala, or dihydroanticapsin). To undertake substrate studies and to couple with purified BacC incubations, we overproduced BacD in *E. coli* BL21 (DE3) cells yielding 6 mg of highly purified BacD per liter of culture (Figure S3).

As expected from the previous published work [10] , BacD supplied with ATP readily ligated L-Tyr onto the *C*-terminus of L-Ala (data not shown). We then found that BacD would ligate L-Ala onto the *N*-terminus of both the 4*S* and 4*R* diastereomers of H_4Tyr, as confirmed by LC/MS (Figures 4B, S10A, and S10B). Given the positive BacC result with only the 4*S*-H_4Tyr diastereomer, we focused our efforts only on this diastereomer and subsequently confirmed the identity of the L-Ala-4*S*-H_4Tyr dipeptide by ^{1}H-NMR (Figure S11A and Table S3). We viewed the L-Ala-4*S*-H_4Tyr dipeptide as a potential substrate for subsequent C_7-hydroxyl oxidation by BacC. However, BacC did not utilize the L-Ala-4*S*-H_4Tyr as a substrate

(Figure S10B). This data strongly argues that the BacC oxidase acts before the BacD ligase in the bacilysin biosynthetic pathway.

Tandem Action of BacC and BacD on 4*S*-H_4Tyr to yield the oxidized dipeptide L-Ala-4*S*-cyclohexenonyl-Ala. Given the oxidoreductase activity of BacC on 4*S*-H_4Tyr and the instability of the BacC enone product, we examined whether the BacD ligase could capture that presumed 4*S*-cyclohexenonyl-Ala BacC product and sweep it through to the dipeptide. A simultaneous incubation of BacC and BacD with 4*S*-H_4Tyr, L-Ala, and ATP did in fact yield the L-Ala-4*S*-cyclohexenonyl-Ala dipeptide product, (Figure 4C), corroborated both by LC/MS (calc.: 253.1194; observed: 253.1198) (Figure S10B) and by ^{1}H-NMR (Figure S11B and Table S4). This result indicates the BacD ligase can intercept the nascent 4*S*-cyclohexenonyl-Ala and ligate its *N*-terminus to L-Ala before its free amino group undergoes intramolecular addition. Although we have not performed comprehensive kinetics with BacD, the fact that the simultaneous BacCD incubations yield predominantly L-Ala-L-cyclohexenonyl-Ala dipeptide and not L-Ala-L-H_4Tyr dipeptide suggests that cyclohexenonyl-Ala is a better substrate than H_4Tyr for the BacD ligase (Figure S10B).

BacC converts dihydroanticapsin to anticapsin in *B. subtilis* Δ*bacC* fermentation extracts. In the aforementioned experiments, we viewed the 4*S*-H_4Tyr diastereomer as a surrogate substrate for BacC and the 4*S*-cyclohexenonyl-Ala BacC oxidation product as a surrogate substrate for BacD ligase. Because we do not currently have a route to purify dihydroanticapsin (with the epoxide intact)

from *ΔbacC* strain extracts, we decided to add exogenous BacC and BacD into crude *ΔbacC* extracts and analyze any dihydroanticapsin transformations by LC/MS.

To supercharge any potential BacC and/or BacD activity, extracts were first doped with 2 mM each of L-Ala, ATP, and NAD^+. The loaded extracts were then exposed to 20 μM of BacC alone, BacD alone, or BacCD simultaneously. LC/MS analysis of these reactions (Figure 5) revealed four important conclusions: 1) BacC oxidizes the C_7-hydroxyl of dihydroanticapsin to generate anticapsin; 2) BacC has no oxidation activity on the dihydrobacilysin dipeptide (as was inferred previously with the L-Ala-4*S*-H_4Tyr dipeptide); 3) BacD can readily ligate dihydroanticapsin with L-Ala to yield dihydrobacilysin; 4) simultaneous BacCD exposure sweeps through dihydroanticapsin to almost exclusively generate bacilysin. These data corroborate our previously drawn conclusion from the surrogate substrates where the tetrahydro amino acid (4*S*-H_4Tyr) was a better substrate for the BacC oxidase than the BacD ligase, and verifies that BacD dipeptide ligation is the last step of bacilysin biosynthesis.

Feeding studies with isotopically labeled [^{13}C]-H_4Tyr and [^{2}H]-H_2HPP. The data we have presented thus far revealed that epoxidation occurs before C_7-hydroxyl oxidation, which occurs before L-Ala ligation. However, it was still not clear at what point epoxidation occurs and if the BacABGF-produced H_4Tyr was an on-pathway intermediate or merely a shunt product. To begin answering these questions, we first prepared mg quantities of 4*S*- and 4*R*-[^{13}C]-H_4Tyr diastereomers (Figures 6A and S6), from 2, 6, 9-[^{13}C]-chorismate utilized in one of our previous

studies [7], 1 millimolar amounts of each of these [^{13}C]-H_4Tyr diastereomers was fed to a small scale growth of *B. subtilis* PY79 WT cells and LC/MS used to detect if any ^{13}C-label was incorporated into bacilysin (Figure S12A). LC/MS analysis showed no increase in the ^{13}C content of detected bacilysin despite the [^{13}C]-H_4Tyr feeding (Figure 6C). This result confirmed our previous suspicion that H_4Tyr is a shunt product and is not on-pathway for bacilysin biosynthesis.

We then decided to go back two enzymatic steps and produce mg quantities of 3*E*- and 3*Z*-[^{2}H]-*ex*-H_2HPP by tandem action of BacAB and AerDE [8], respectively, in D_2O (= ^2H_2O) (Figures S6A and S6C). (We chose ^{13}C-labeling of the H_4Tyr diastereomers in the above paragraph because running the 4-enzyme tandem of either BacABGF or AerDE + BacGF in D_2O was severely inefficient due to cumulative solvent isotope effects.) When the [^{13}C]-H_4Tyr feeding described above was carried out instead with the [$^2H_2$]-*ex*-H_2HPP diastereomers, LC/MS analysis revealed that deuterons from 3*E*-*ex*-H_2HPP (and less so 3*Z*-*ex*-H_2HPP) appeared in bacilysin upon *B. subtilis* WT fermentation (Figures 6D and S12B and Table S5). (We did not expect the results of this feeding to be perfectly clean as we have previously shown that BacB can interconvert the 3*E*- and 3*Z*-*ex*-H_2HPP isomers [7].) To confirm this result we fed the [^{2}H]-*ex*-H_2HPP diastereomers to the *B. subtilis ΔbacC* deletion strain and were able to detect deuterons primarily from 3*E*-*ex*-H_2HPP in both dihydroanticapsin and dihydrobacilysin (Figures 7 and S13). This result was initially baffling because our previous experiments clearly demonstrated that the 3*Z* (and not the 3*E*) diastereomer undergoes BacG-mediated hydride reduction to give the 4*S* stereochemistry that is seen in anticapsin/bacilysin (Figure 1) [8, 18, 21]. A

probable explanation for this result is that 3*E*-*ex*-H_2HPP is the substrate for epoxidation by a currently unidentified enzyme activity in the pathway.

In addition to the *ΔbacC B. subtilis* PY79 strain, we also possessed a *ΔbacB* deletion strain constructed by equivalent methodology that has been previously reported [13] . When *bacB* was deleted there was no detectable production of anticapsin, bacilysin, or dihydro intermediates (found in the *ΔbacC* strain) in the fermentation extracts (Figures S9A and S9B). This result is consistent with BacB playing an essential, but earlier role than BacC in the anticapsin/bacilysin pathway. Indeed, when the *B. subtilis* PY79 *ΔbacB* strain was fed with the [^{2}H]-*ex*-H_2HPP diastereomers, neither the 3*E* nor the 3*Z* isomer rescued bacilysin/anticapsin/dihydroanticapsin production (data not shown). As a member of the bicupin enzyme family, which are known to possess a wide range of activities [22, 23] , it is possible that BacB is the missing epoxidase [24] although our assays with purified BacB have not revealed such an activity.

Proposed Biosynthetic Pathway to Anticapsin and Bacilysin. Given the results from the studies described here and building on prior efforts [6-8] , we can fill in missing steps in the anticapsin/bacilysin pathway and show that BacC and BacD catalyze the last two steps. In particular BacC is a NAD^+-dependent alcohol dehydrogenase, working to oxidize the C_7-hydroxyl as the last step in anticapsin assembly (Figure 8). BacD is the dipeptide ligase that adds L-Ala to the amino group of anticapsin as a self-protection strategy of *B. subtilis* producers against inactivation of their own glucosamine synthase by anticapsin. BacD is promiscuous

for the *C*-terminal substrate, also accepting 2*S*-Tyr, 2*S*, 4*R*, 7*R*- and 2*S*, 4*S*, 7*R*-H_4Tyr diastereomers, and also dihydroanticapsin for coupling with L-Ala.

Our previous efforts [7, 25] have defined BacA as the founding member of a novel class of non-aromatizing prephenate decarboxylases that initiates the pathway by diverting some of the prephenate pool to the endocyclic dienyl product 7*R*-*en*-H_2HPP. BacB acts next to accelerate the isomerization of one of the double bonds into conjugation with the 2-keto moiety to yield the thermodynamically favored 7*R*-exocyclic-H_2HPP. We have demonstrated that BacB equilibrates the Δ^3-geometric isomers to a 7:3 *E*:*Z* ratio [7].

Two findings of this study are consistent with epoxidation of the double-bond occurring next, by an as yet uncharacterized enzyme activity. One of those findings is that 3*E*-H_2HPP (but not 3*Z*) is on pathway (deduced from feeding studies) in the parental *B. subtilis* strain and in a *ΔbacC* but not a *ΔbacB* strain. The second finding is that dihydroanticapsin accumulates in the *ΔbacC* strain and can be processed by pure BacC and then BacD to anticapsin and bacilysin, respectively.

We thus feature epoxidation occurring at the level of the 3*E*-*ex*-H_2HPP isomers. Epoxidation after reduction to the 4*S*-H_4HPP level is ruled out by failure of the 3*Z*-H_2HPP isomer (known to give 4*S*-H_4HPP by BacG action [8]) to yield anticapsin/bacilysin in the feeding studies noted above. We further posit that *in vitro* action of BacG and BacF on the 3*E*- and 3*Z*-H_2HPP isomers [8] reflects the permissiveness of these reactants as surrogate substrates. The resultant H_4Tyr diastereomers are shunt products (and in labeled form do not go on to anticapsin)

but the stereochemical outcome from BacG action [8] is a useful constraint: 3*E*-*ex*-H_2HPP gives the 4*R*-H_4Tyr product (after coupled transamination by BacF) while 3*Z*-*ex*-H_2HPP gives the 4*S*-H_4Tyr product. Anticapsin (and by inference dihydroanticapsin) has 4*S*-stereochemistry. Thus, a putative epoxy-H_2HPP substrate for BacG could be the 3*Z*- isomer with the same facial selectivity for hydride addition to C_4. This would suggest BacB could equilibrate the epoxy-3*E*-H_2HPP to the 3*Z* isomer before BacG acts (Path 2 in Figure 8). Alternatively, the prior introduction of the epoxy group on the 3*E* isomer could direct hydride addition by BacG preferentially/exclusively to the ring face opposite to the epoxide (Path 1) and yield epoxy-4*S*-H_4HPP, a transamination away from the observed dihydroanticapsin (Figures S2C and S2D). Further insights will require detection of the earliest epoxygenated scaffold and the catalyst responsible.

With regard to antibiotic activity, we compared bacilysin with dihydrobacilysin as noted in Figure S14B against a lawn of *S. aureus* RN4220 as the test organism. Bacilysin releases the proximal inhibitor anticapsin and has the anticipated growth inhibition. Dihydrobacilysin is inactive in that initial assay, most probably because dihydroanticapsin, while possessing the epoxide, lacks the C_7 ketone functionality, implicated in the glucosamine synthetase inactivation mechanism by Baldwin and colleagues [4]. In terms of the importance of the epoxide to the epoxyketone warhead, we found that the L-Ala-4*S*-cyclohexenonyl-Ala dipeptide described above from action of BacC and BacD on L-Ala and 2*S*, 4*S*, 7*R*-H_4Tyr also does not show antibiotic activity under those assay conditions (Figure S14A). Future efforts will be required to deconvolute whether the 4*S*-

cyclohexenonyl-Ala is released by peptidase action in the target bacterial cell, lasts long enough to reach the active site of glucosamine synthase, and whether the enone is or is not an effective warhead compared to the epoxyketone in anticapsin.

ACKNOWLEDGEMENTS

We thank Dr. Sarah A. Mahlstedt for construction of the *B. subtilis* PY79 Δ*bacB* deletion strain and for helpful discussions. We thank Dr. Daniel Kearns (Indiana University) for the generous gift of the pMiniMAD plasmid used to construct the *B. subtilis* genomic deletion strains used in this work and Dr. David Rudner (HMS) for technical advice on its use. LC/MS data were acquired using an Agilent 6520 spectrometer purchased using Taplin Funds. We also thank Dr. Timothy A. Wencewicz for helpful advice and discussions.

SUPPORTING INFORMATION AVAILABLE

Mechanism of glutaminase domain of glucosamine synthetase; proposed BacG mechanism with epoxy-3*E*-*ex*-H_2HPP; SDS-PAGE analysis of BacC and BacD; schematic of gene deletion via pMiniMAD plasmid; ^{1}H-NMR spectra of formate spiked H_4Tyr isomers; isotopic labeling patterns of [^{13}C]-H_4Tyr and [^{2}H]-*ex*-H_2HPP isomers; isotopic labeling of bacilysin from 3-[^{13}C]-L-Ala feeding; LC/MS pattern of bacilysin from [^{2}H]-*ex*-H_2HPP feeding under alternative growth conditions; ion-extracted LC/MS spectra of *B. subtilis* PY79 WT, Δ*bacB*, and Δ*bacC* Dowex processed media extracts; LC/MS ion-extractions of BacC/BacD incubations with H_4Tyr isomers; ^{1}H-NMR assignments and tabulated data for L-Ala-4*S*-H_4Tyr and L-Ala-4*S*-cyclohexenonyl-Ala dipeptides; predicted isotopic label transfers from [^{13}C]-H_4Tyr

and [^{2}H]-*ex*-H_2HPP isomers to bacilysin; LC/MS data of dihydrobacilysin/dihydroanticapsin obtained from Dowex purification of *B. subtilis* PY79 Δ*bacC* extract with [^{2}H]-*ex*-H_2HPP feeding; antibiotic assays against *S. aereus* RN4220; ^{1}H-NMR spectrum of bacilysin; and DNA oligonucleotide primers used for pMiniMAD constructs. This material is available free of charge via the Internet at http://pubs.acs.org.

REFERENCES

(1) Steinborn, G.; Hajirezaei, M.; Hofemeister, J. (2005) *bac* genes for recombinant bacilysin and anticapsin production in *Bacillus* host strains. *Arch. Microbiol. 183*, 71-79.

(2) Perry, D.; Abraham, E. P. (1979) Transport and metabolism of bacilysin and other peptides by suspensions of *Staphylococcus aureus*. *J. Gen. Microbiol. 115*, 213-221.

(3) Milewski, S.; Chmara, H.; Borowski, E. (1986) Anticapsin - an active-site directed inhibitor of glucosamine-6-phosphate synthetase from *Candida albicans*. *Drugs Exp. Clin. Res. 12*, 577-583.

(4) Baldwin, J. E.; Adlington, R. M.; Mitchell, M. B. (1995) Stereocontrolled enantiospecific synthesis of anticapsin. *Tetrahedron 51*, 5193-5206.

(5) Inaoka, T.; Takahashi, K.; Ohnishi-Kameyama, M.; Yoshida, M.; Ochi, K. (2003) Guanine nucleotides guanosine 5 '-diphosphate 3 '-diphosphate and GTP co-operatively regulate the production of an antibiotic bacilysin in *Bacillus subtilis*. *J. Biol. Chem. 278*, 2169-2176.

(6) Mahlstedt, S. A.; Walsh, C. T. (2010) Investigation of anticapsin biosynthesis reveals a four-enzyme pathway to tetrahydrotyrosine in *Bacillus subtilis*. *Biochemistry 49*, 912-923.

(7) Parker, J. B.; Walsh, C. T. (2012) Olefin isomerization regiochemistries during tandem action of BacA and BacB on prephenate in bacilysin biosynthesis. *Biochemistry (N. Y.) 51*, 3241-3251.

(8) Parker, J. B.; Walsh, C. T. (2012) Stereochemical outcome at four stereogenic centers during conversion of prephenate to tetrahydrotyrosine by BacABGF in the bacilysin pathway. *Biochemistry (N. Y.) 51*, 5622-5632.

(9) Hilton, M.; Alaeddinoglu, N.; Demain, A. (1988) Synthesis of bacilysin by *Bacillus-subtilis* branches from prephenate of the aromatic amino-acid pathway. *J. Bacteriol. 170*, 482-484.

(10) Shomura, Y.; Hinokuchi, E.; Ikeda, H.; Senoo, A.; Takahashi, Y.; Saito, J.; Komori, H.; Shibata, N.; Yonetani, Y.; Higuchi, Y. (2012) Structural and enzymatic characterization of BacD, an L-amino acid dipeptide ligase from *Bacillus subtilis*. *Protein Science 21*, 707-716.

(11) Tabata, K.; Ikeda, H.; Hashimoto, S. (2005) *ywfE* in *Bacillus subtilis* codes for a novel enzyme, L-amino acid ligase. *J. Bacteriol. 187*, 5195-5202.

(12) Chen, R.; Guttenplan, S. B.; Blair, K. M.; Kearns, D. B. (2009) Role of the sigma(D)-dependent autolysins in *Bacillus subtilis* population heterogeneity. *J. Bacteriol. 191*, 5775-5784.

(13) Mahlstedt, S. A. (2011) *Novel Routing of Prephenate to Natural Products*. Harvard University.

(14) Gibson, D. G.; Young, L.; Chuang, R.; Venter, J. C.; Hutchison, Clyde A.,,III; Smith, H. O. (2009) Enzymatic assembly of DNA molecules up to several hundred kilobases. *Nature Methods 6*, 343-345.

(15) Walker, J.; Abraham, E. (1970) Isolation of bacilysin and a new amino acid from culture filtrates of *Bacillus subtilis*. *Biochem. J. 118*, 557-561.

(16) Pollock, M.; Kramer, M. (1958) Intermediates in the biosynthesis of bacterial penicillinase. *Biochem. J. 70*, 665-681.

(17) Gottlieb, H.; Kotlyar, V.; Nudelman, A. (1997) NMR chemical shifts of common laboratory solvents as trace impurities. *J. Org. Chem. 62*, 7512-7515.

(18) Wild, H. (1994) Enantioselective total synthesis of the antifungal natural-products chlorotetaine, bacilysin, and anticapsin and of related-compounds - Revision of the relative configuration. *J. Org. Chem. 59*, 2748-2761.

(19) Lifshits, M.; Carmeli, S. (2012) Metabolites of *Microcystis aeruginosa* bloom material from Lake Kinneret, Israel. *J. Nat. Prod. 75*, 209-219.

(20) Ishida, K.; Christiansen, G.; Yoshida, W. Y.; Kurmayer, R.; Welker, M.; Valls, N.; Bonjoch, J.; Hertweck, C.; Boerner, T.; Hemscheidt, T.; Dittmann, E. (2007) Biosynthesis and structure of Aeruginoside 126A and 126B, cyanobacterial peptide glycosides bearing a 2-carboxy-6-hydroxyoctahydroindole moiety. *Chem. Biol. 14*, 565-576.

(21) Baldwin, J.; Adlington, R.; Mitchell, M. (1993) Stereocontrolled enantiospecific synthesis of anticapsin - Revision of the configuration. *Journal of the Chemical Society-Chemical Communications* 1332-1335.

(22) Agarwal, G.; Rajavel, M.; Gopal, B.; Srinivasan, N. (2009) Structure-based phylogeny as a diagnostic for functional characterization of proteins with a Cupin fold. *Plos One 4*, e5736.

(23) McLuskey, K.; Cameron, S.; Hammerschmidt, F.; Hunter, W. (2005) Structure and reactivity of hydroxypropylphosphonic acid epoxidase in fosfomycin biosynthesis by a cation- and flavin-dependent mechanism. *Proc. Natl. Acad. Sci. U. S. A. 102*, 14221-14226.

(24) Rajavel, M.; Mitra, A.; Gopal, B. (2009) Role of *Bacillus subtilis* BacB in the synthesis of bacilysin. *J. Biol. Chem. 284*, 31882-31892.

(25) Mahlstedt, S.; Fielding, E. N.; Moore, B. S.; Walsh, C. T. (2010) Prephenate decarboxylases: a new prephenate-utilizing enzyme family that performs nonaromatizing decarboxylation en route to diverse secondary metabolites. *Biochemistry 49*, 9021-9023.

FIGURE LEGENDS

Figure 1. (A) Proposed biosynthetic pathway from prephenate to the dipeptide antibiotic bacilysin via a previously identified *ex*-H_2HPP intermediate. Dashed arrow represents the unknown identity of the proposed expoxidase. (B) BacABGF action on prephenate yields two diastereomers of H_4Tyr with differing stereochemistry at the C_4 position. (Inset) Proposed bacilysin biosynthetic gene cluster present in *B. subtilis* PY79.

Figure 2. (A) Structures and calculated masses of bacilysin and its warhead, anticapsin, along with their dihydro-counterparts. (B) Extracted ion traces (+/- 0.002 *m/z* tolerance) of anticapsin, dihydroanticapsin, bacilysin, and dihydrobacilysin from LC/MS runs (positive detection mode) of media extracts (without Dowex processing) from *B. subtilis* PY79 wild-type (WT) and Δ*bacC* strain growths. (C) Observed masses of the compounds highlighted in (B).

Figure 3. Incubation of dihydroanticapsin (a proposed bacilysin intermediate) with BacC and NAD^+ cofactor yields anticapsin. Exposure of dihydroanticapsin to acid (H^+) opens the epoxide and forms the hydrate of dihydroanticapsin (5, 6, 7-trihydroxycyclohexyl-Ala). Dihydroanticapsin hydrate is no longer a substrate for BacC. (Inset) Assigned ^{1}H-NMR spectrum for dihydroanticapsin hydrate.

Figure 4. (A) Kinetic traces (340 nm UV absorbance) monitoring NADH formation produced from the action of BacC with NAD^+ cofactor on the substrates 4*S*- and 4*R*-H_4Tyr. (B) BacD ligase action with L-alanine, ATP cofactor, and either 4*S*- or 4*R*-H_4Tyr readily produces dipeptide with L-Ala at the *N*-terminus. (C) The coupled

action of BacC and BacD (simultaneous incubation with appropriate cofactors) utilizes the 4*S* diastereomer of H_4Tyr to yield the dipeptide L-Ala-2*S*, 4*S*-cyclohexenonyl-Ala.

Figure 5. Extracted ion traces (+/- 0.002 *m/z* tolerance) of anticapsin, dihydroanticapsin, bacilysin, and dihydrobacilysin from LC/MS runs (positive detection mode) of media extract from *B. subtilis* PY79 Δ*bacC* cells (without Dowex processing) after incubation with and without exogenous BacC and BacD (exogenous cofactors/substrate ATP, NAD^+, and L-Ala included in each incubation).

Figure 6. (A) Schematic showing labeled positions in non-uniformly ^{13}C enriched 4*R*- and 4*S*-H_4Tyr used for feeding studies. (B) Schematic showing deuterated (^2H = D) positions in deuterium enriched 3*E*- and 3*Z*-*ex*-H_2HPP from BacAB and AerDE incubations, respectively. (C) Comparative mass spectra profiles of bacilysin obtained from analysis of media extracts (without Dowex processing) produced by *B. subtilis* PY79 WT cells with and without feeding of [^{13}C]-H_4Tyr diastereomers in (A). (D) Comparative mass spectra profiles of bacilysin obtained from analysis of media extracts produced by *B. subtilis* PY79 WT cells with and without feeding of [^2H]-*ex*-H_2HPP diastereomers in (B).

Figure 7. (A) Structure and calculated mass of dihydroanticapsin. (B) Structure and calculated mass of dihydrobacilysin. (C) Comparative mass spectra profiles of dihydroanticapsin obtained from media extracts (without Dowex processing) produced by *B. subtilis* PY79 Δ*bacC* cells with and without feeding of [^2H]-3*E*-*ex*-H_2HPP. (D) Comparative mass spectra profiles of dihydrobacilysin obtained from

media extracts (without Dowex processing) produced by *B. subtilis* PY79 Δ*bacC* cells with and without feeding of [^{2}H]-3*E*-*ex*-H_2HPP.

Figure 8. Detailed schematic showing the newly hypothesized biosynthetic pathway from prephenate to bacilysin. The identity of the epoxidase remains unknown and the proposed epoxyketo-acids have not yet been detected.

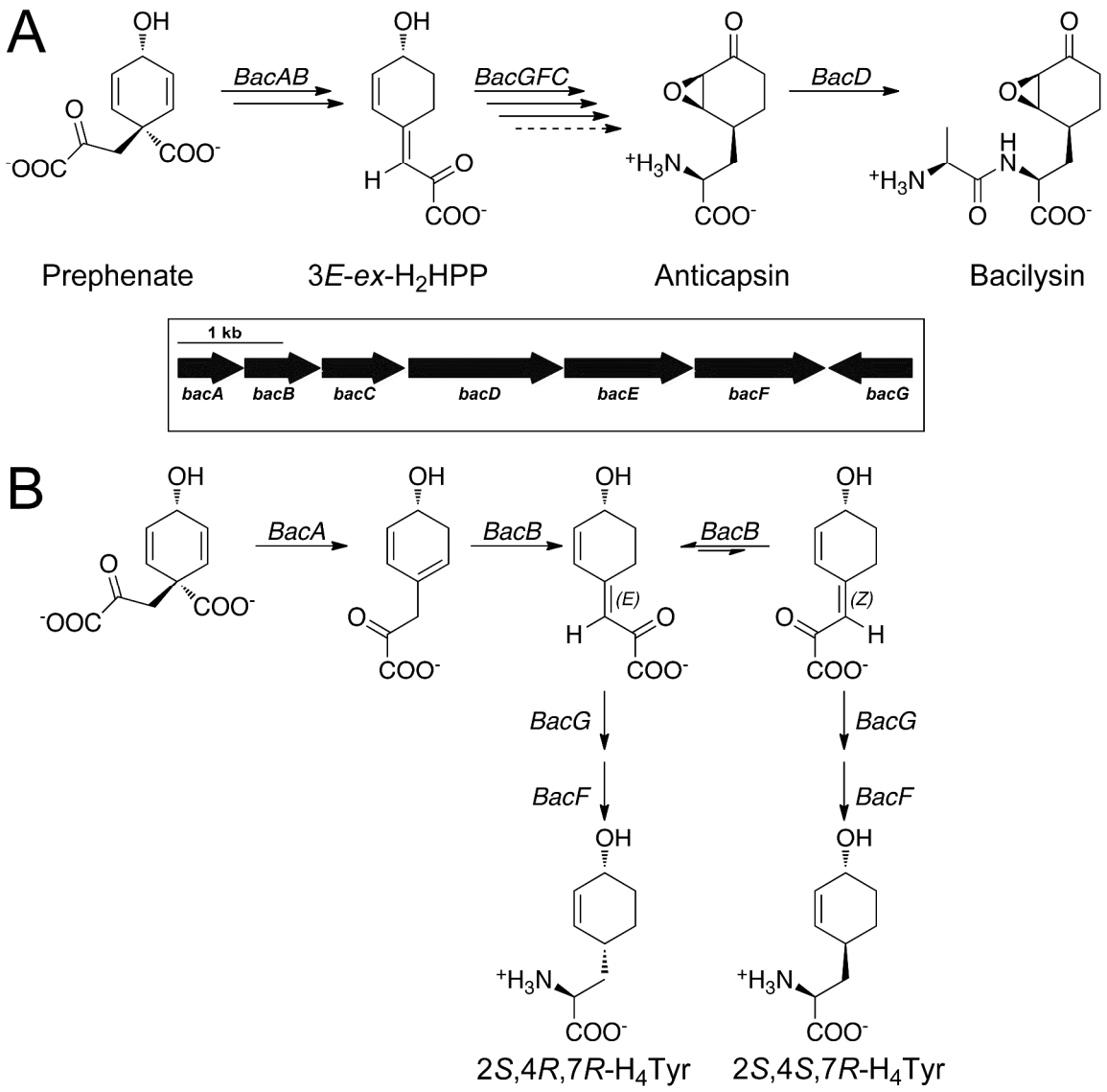
A
BacAB
BacGFC
BacD
Prephenate
3E-ex-H2HPP
Anticapsin
Bacilysin
1 kb
bacA
bacB
bacC
bacD
bacE
bacF
bacG
B
BacA
BacB
BacB
(E)
(Z)
BacG
BacF
BacG
BacF
2S,4R,7R-H4Tyr
2S,4S,7R-H4Tyr

Figure 1

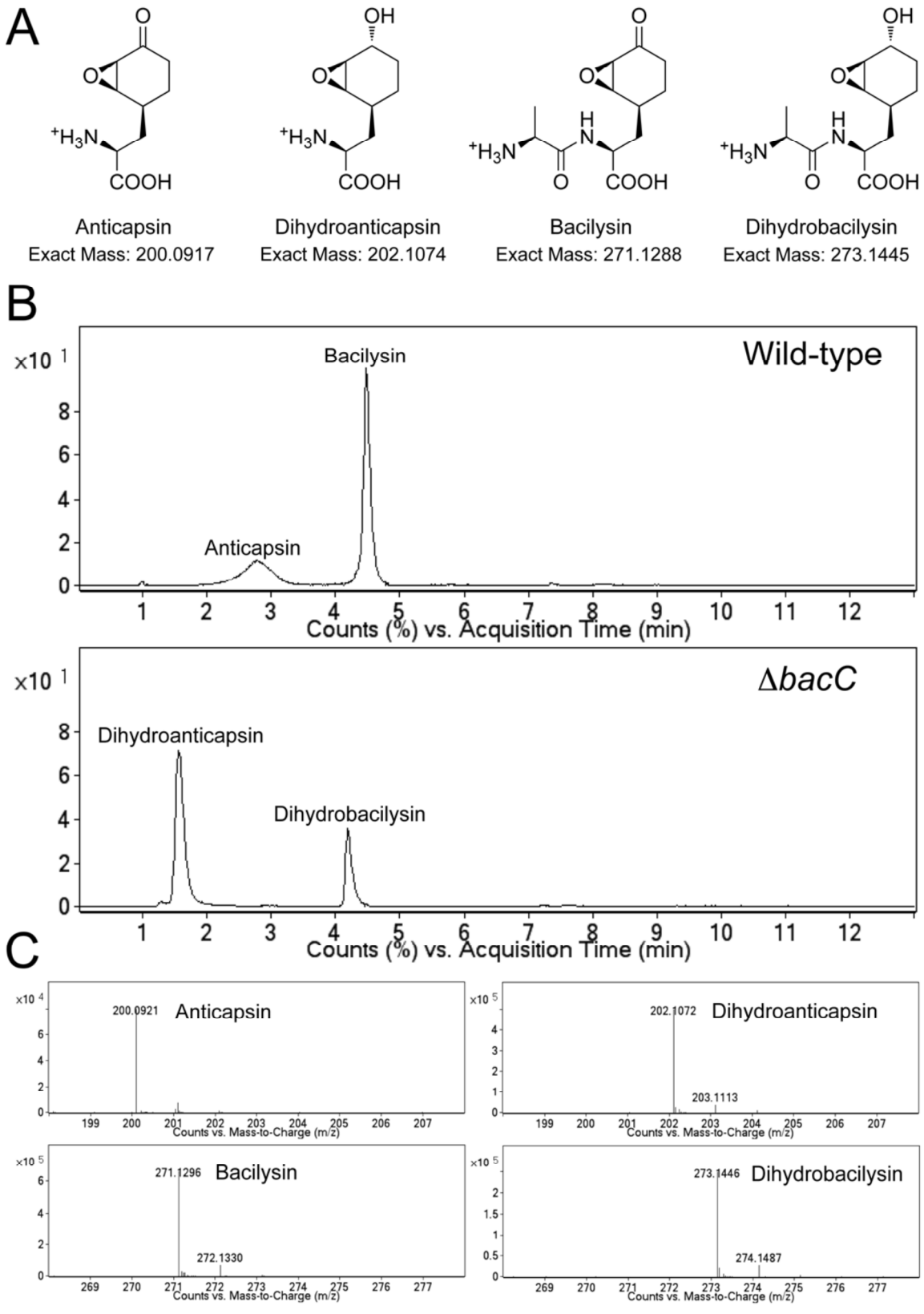
A
Anticapsin
Exact Mass: 200.0917
Dihydroanticapsin
Exact Mass: 202.1074
Bacilysin
Exact Mass: 271.1288
Dihydrobacilysin
Exact Mass: 273.1445
B
Wild-type
Bacilysin
Anticapsin
Counts (%) vs. Acquisition Time (min)
ΔbacC
Dihydroanticapsin
Dihydrobacilysin
Counts (%) vs. Acquisition Time (min)
C
200.0921 Anticapsin
202.1072 Dihydroanticapsin
203.1113
271.1296 Bacilysin
272.1330
273.1446 Dihydrobacilysin
274.1487
Counts vs. Mass-to-Charge (m/z)

Figure 2

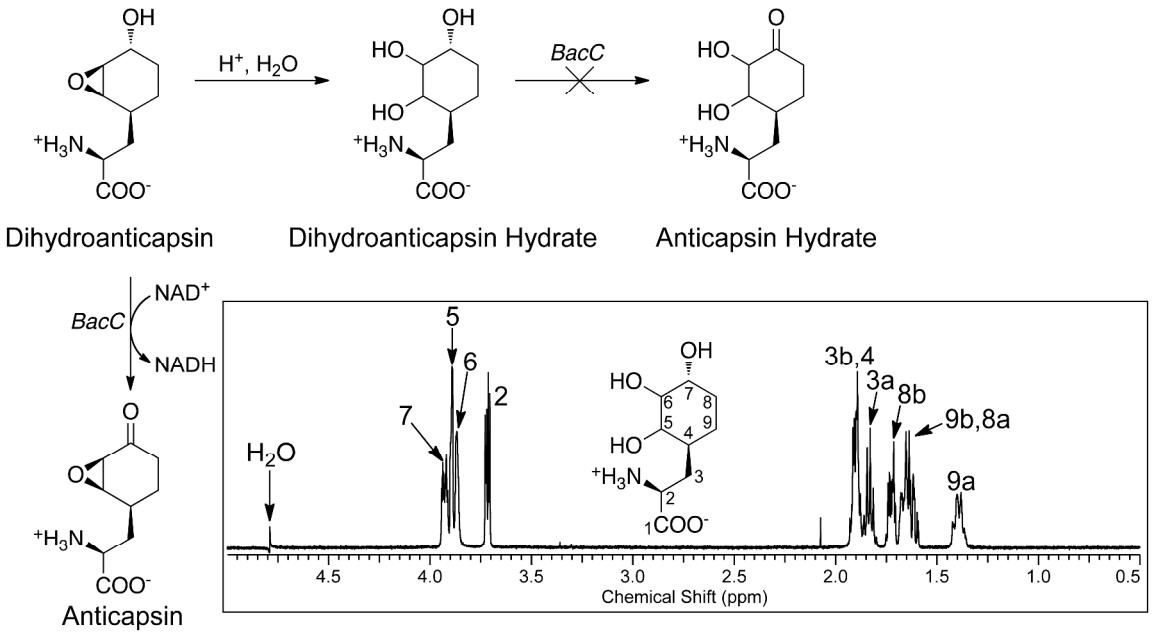
OH
O
+H3N
COO-
H+, H2O
HO
BacC
Dihydroanticapsin
Dihydroanticapsin Hydrate
Anticapsin Hydrate
NAD+
NADH
Anticapsin
H2O
5
6
7
2
3b,4
3a
8b
9b,8a
9a
4.5
4.0
3.5
3.0
2.5
2.0
1.5
1.0
0.5
Chemical Shift (ppm)

Figure 3

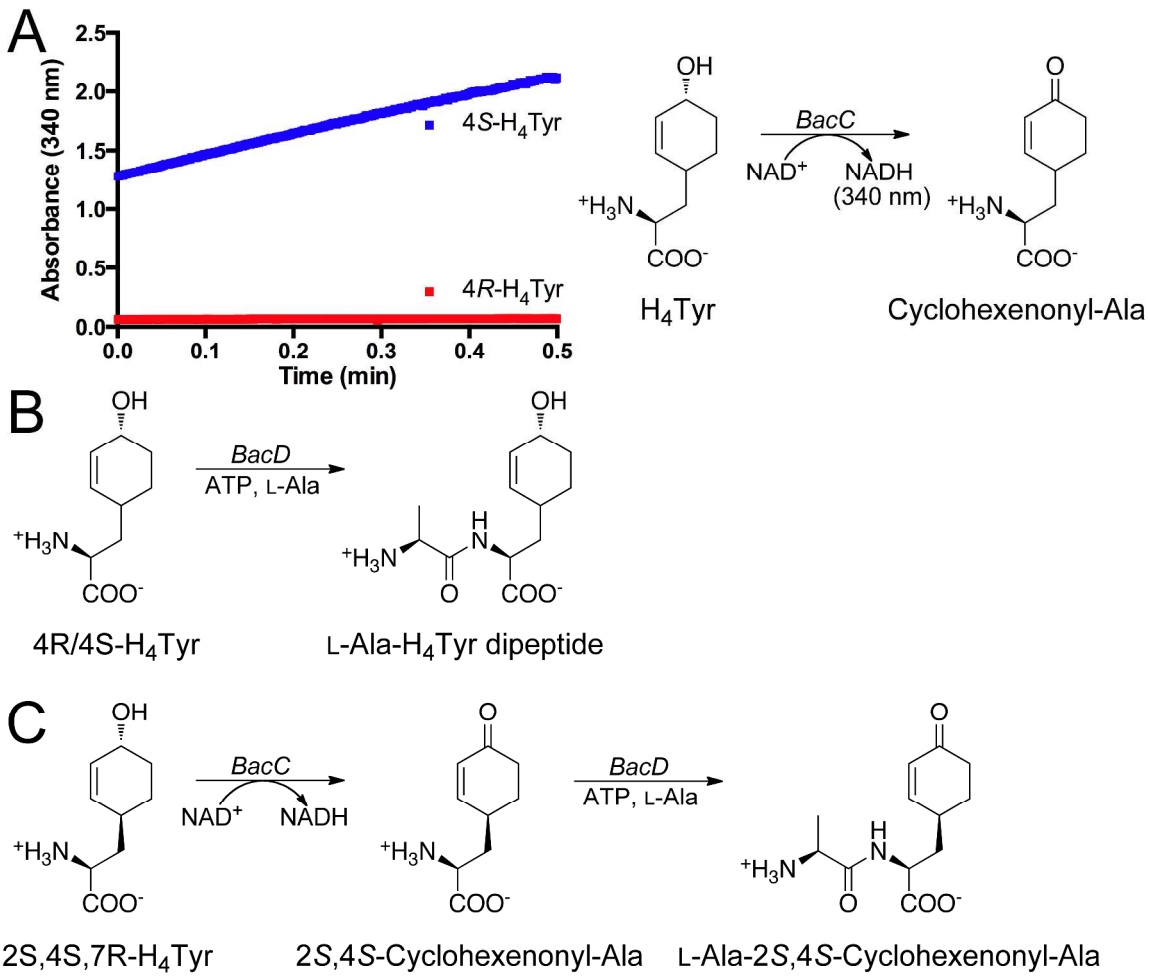
A
Absorbance (340 nm)
Time (min)
4S-H4Tyr
4R-H4Tyr
BacC
NAD+
NADH
(340 nm)
H4Tyr
Cyclohexenonyl-Ala
B
BacD
ATP, L-Ala
4R/4S-H4Tyr
L-Ala-H4Tyr dipeptide
C
BacC
NAD+
NADH
BacD
ATP, L-Ala
2S,4S,7R-H4Tyr
2S,4S-Cyclohexenonyl-Ala
L-Ala-2S,4S-Cyclohexenonyl-Ala

Figure 4

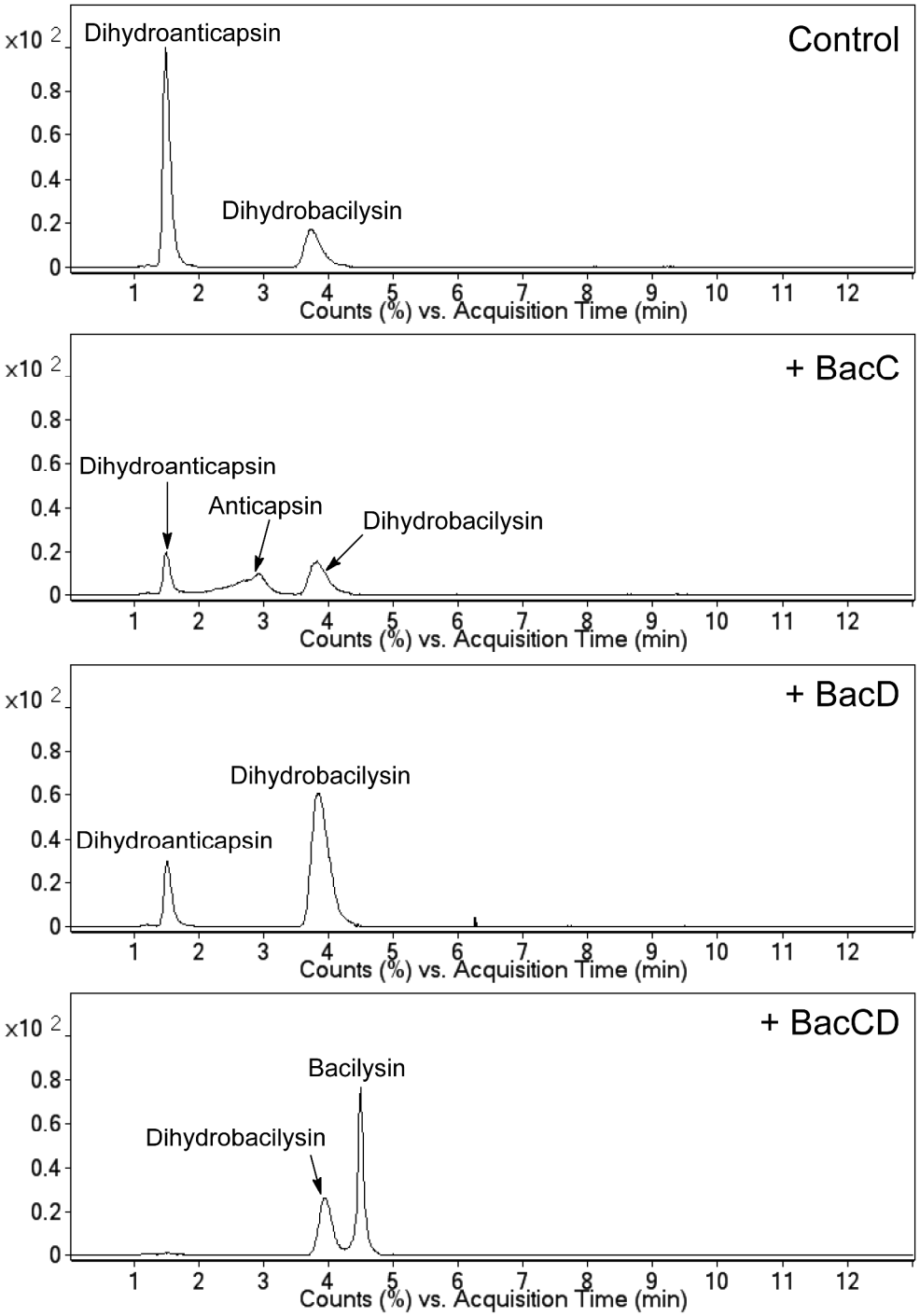
x10 2
Dihydroanticapsin
Control
Dihydrobacilysin
Counts (%) vs. Acquisition Time (min)
+ BacC
Anticapsin
+ BacD
+ BacCD
Bacilysin

Figure 5

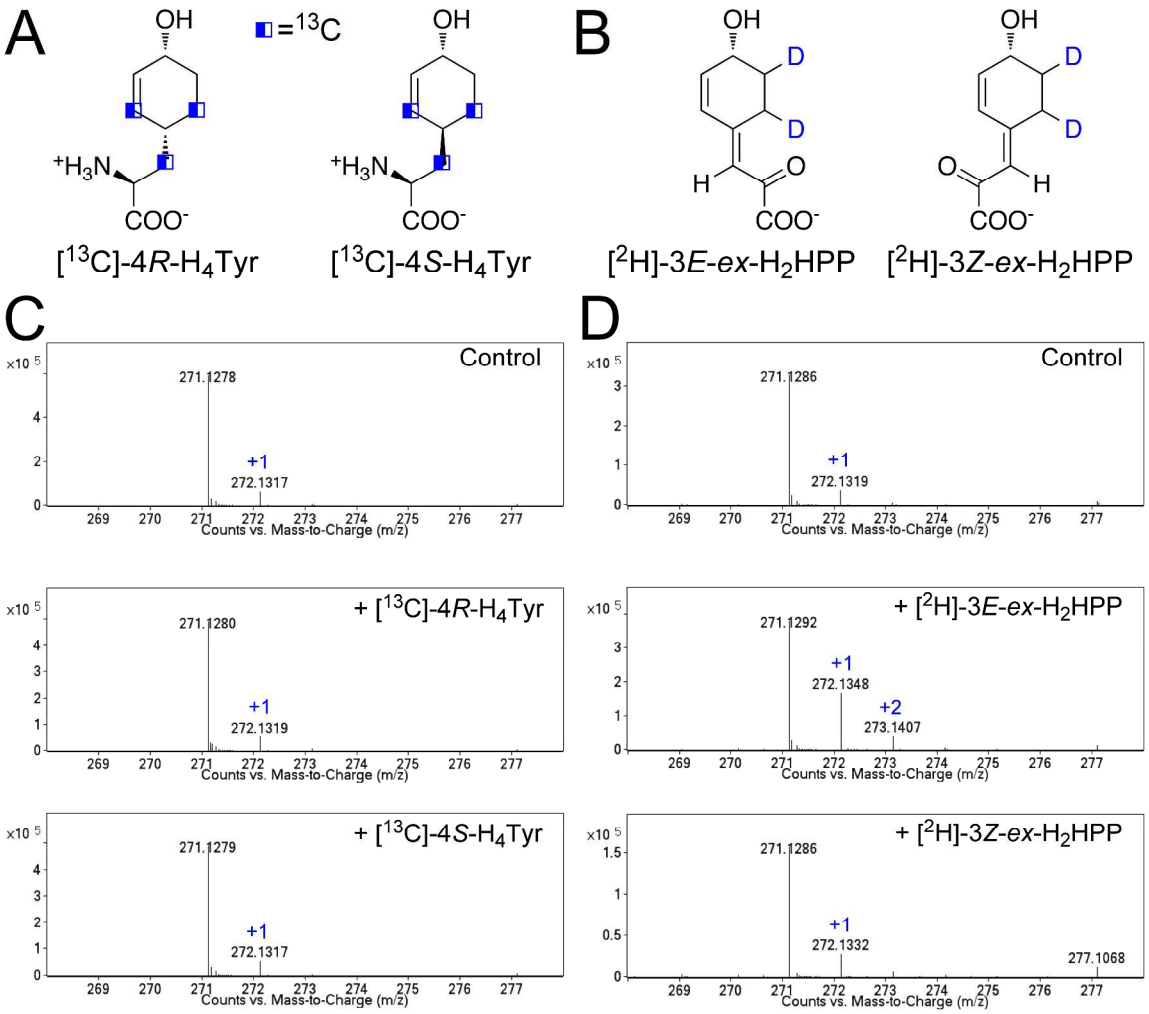
A
=13C
OH
+H3N
COO-
[13C]-4R-H4Tyr
[13C]-4S-H4Tyr
B
D
O
H
[2H]-3E-ex-H2HPP
[2H]-3Z-ex-H2HPP
C
D
Control
271.1278
+1
272.1317
271.1286
272.1319
+ [13C]-4R-H4Tyr
271.1280
272.1319
+ [2H]-3E-ex-H2HPP
271.1292
272.1348
+2
273.1407
+ [13C]-4S-H4Tyr
271.1279
272.1317
+ [2H]-3Z-ex-H2HPP
271.1286
272.1332
277.1068
Counts vs. Mass-to-Charge (m/z)

Figure 6

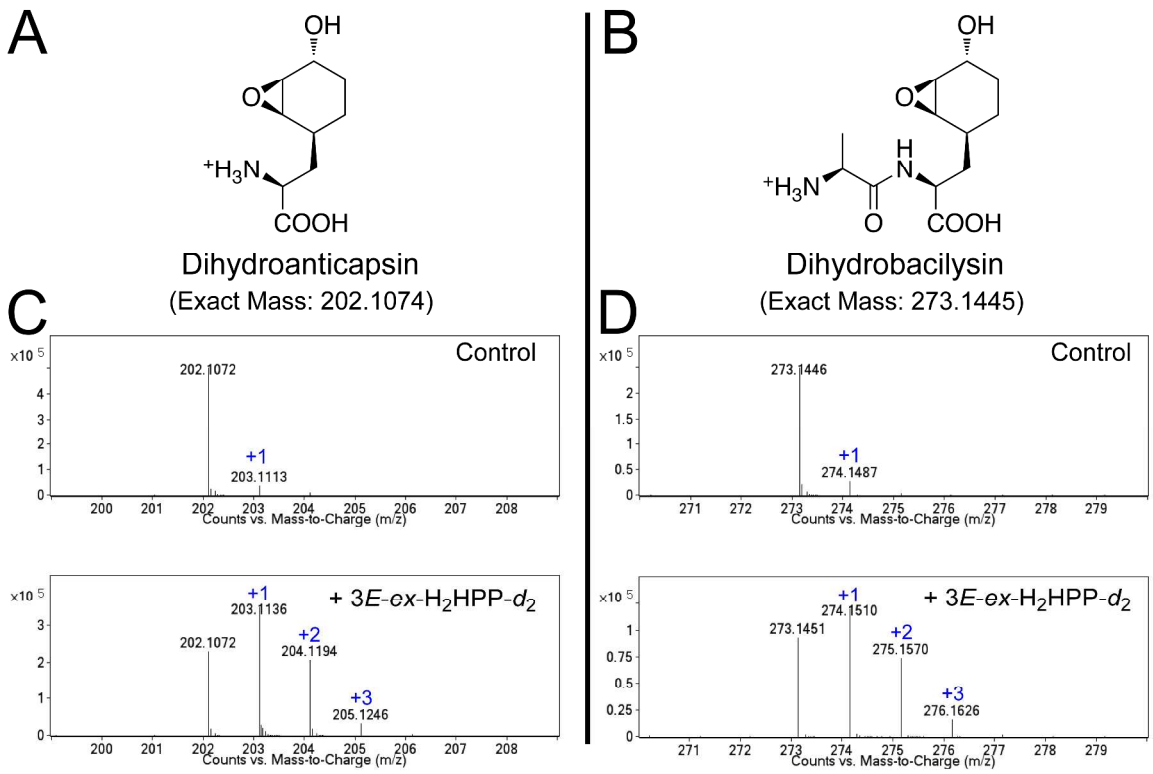
A
OH
O
+H3N
COOH
Dihydroanticapsin
(Exact Mass: 202.1074)
B
OH
O
H
N
+H3N
O
COOH
Dihydrobacilysin
(Exact Mass: 273.1445)
C
Control
202.1072
+1
203.1113
Counts vs. Mass-to-Charge (m/z)
+1
203.1136
+ 3E-ex-H2HPP-d2
202.1072
+2
204.1194
+3
205.1246
Counts vs. Mass-to-Charge (m/z)
D
Control
273.1446
+1
274.1487
Counts vs. Mass-to-Charge (m/z)
+1
274.1510
+ 3E-ex-H2HPP-d2
273.1451
+2
275.1570
+3
276.1626
Counts vs. Mass-to-Charge (m/z)

Figure 7

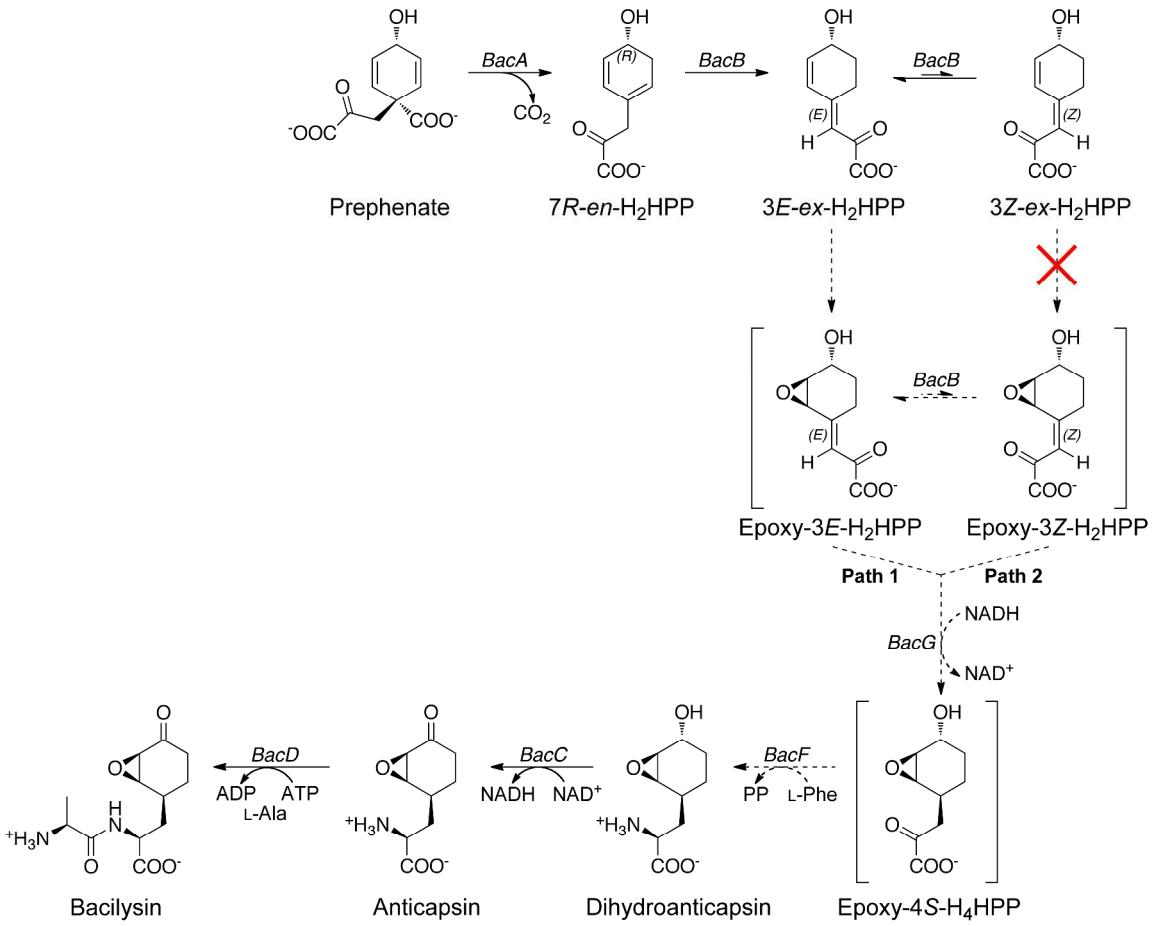
Prephenate
BacA
CO2
7R-en-H2HPP
BacB
3E-ex-H2HPP
BacB
3Z-ex-H2HPP
BacB
Epoxy-3E-H2HPP
Epoxy-3Z-H2HPP
Path 1
Path 2
BacG
NADH
NAD+
Epoxy-4S-H4HPP
BacF
PP
L-Phe
Dihydroanticapsin
BacC
NADH
NAD+
Anticapsin
BacD
ADP
ATP
L-Ala
Bacilysin

Figure 8

For Table of Contents Use Only

Action and Timing of BacC and BacD in the Late Stages of Biosynthesis of the Dipeptide Antibiotic Bacilysin

Jared B. Parker and Christopher T. Walsh